Skirt Material Effects on Air Cushion Dynamic Heave Stability

T. A. Graham,* P. A. Sullivan,† and M. J. Hinchey‡
University of Toronto, Downsview, Canada

An investigation of the effects of the viscoelastic properties of flexible skirt material on the dynamic stability of a plenum chamber air cushion is described. The skirt is a slightly tapered cone, and two materials used for building laboratory-scale models are tested. Dynamic uniaxial tension tests are used to obtain the viscoelastic parameters. A linear stability analysis of the heave dynamics is based on the usual lumped capacitance model, but is modified to include the effect of skirt deformation on cushion volume and hovergap. Large changes in the stability characteristics from those of an inelastic cushion are predicted. The experiments confirm the predictions, and it is concluded that great care has to be exercised in the choice of model skirt material.

Nomenclature

a = atmospheric sound speed
A_b = area of vehicle planform as reference in calculating C_{QC} and C_{SW}, for conical cell, $=(\pi/4)D_{st}^2$
A_d = cross-sectional area of duct
C_c = cushion capacitance, $= V_{ce}/\rho a^2$
C_m = discharge coefficient in cushion air escape law
C_{mi} = flow coefficient for duct inlet
C_{PC} = cushion pressure coefficient, $= p_{ce}/P_a$
C_{QC} = cushion flow coefficient, $C_{QC} = Q_e(\rho/2WA_{\text{base}})^{1/2}$
C_{SW} = $w_s A_b / W$
d_r = D_{sb}/D_{sm}
D_{in} = cushion inlet diameter
D_{sb} = diameter of conical skirt at lip
D_{sm} = mean diameter of conical skirt
D_{st} = diameter of skirt at top
E_1, E_2 = storage and loss modulus characterizing response of material to oscillating strains
E, E_g, E_v = spring coefficients in phenomenological material models (E = Young's modulus, E_g = spring element in series with Voigt element to make standard linear model, E_v = spring element of Voigt model)
g = acceleration due to gravity
h = hovergap
h_s = height of skirt, see Fig. 2
ℓ_ℓ = length of perimeter of skirt at lip
ℓ_s = mean length of skirt perimeter
L_d = duct length
p_c = cushion gage pressure
p_{df} = pressure in the duct at conical inlet
p_f = equivalent fan or source pressure
P_a = absolute atmospheric pressure
Q_a = volume flux past cushion lip to atmosphere
Q_d = volume flux through duct
r_c = radius of curved region at top of skirt
s = slant length of skirt
S_a = cushion support area
t = time
t_s = thickness of skirt material
V_a = cushion "active" volume, $= S_a h$
V_c = total cushion volume
V_d = cushion "dead" volume
w_s = weight per unit area of skirt material
W = gross weight supported by cushion
x = height of cushion base above ground
γ = isentropic exponent
δ = material loss angle, $\tan\delta = E_1/E_2$
ϵ = strain
η = material damping coefficient
θ = skirt taper angle
ν = Poisson's ratio
ν_e = skirt contraction coefficient
ρ = air density
σ = stress
ω = angular frequency

Subscripts

e = equilibrium value
h = hoop direction
0 = undeformed quantities

Introduction

THE success of all modern air cushion vehicles (ACV) depends largely on the use of flexible skirts to permit negotiation of obstacles or waves while retaining relatively low levitation power or hovergap. A skirt is a collapsible structure inflated and stabilized by the pressure of the cushion air and is usually made from a woven fabric coated with an elastomer. Such composite materials can possess nonlinear, viscoelastic and anisotropic properties. It is of fundamental interest to ascertain the effect of these properties on the dynamics of the vehicle, both at full scale and for test models. Although detailed analyses of ACV cushion and skirt dynamics are now appearing in the open literature (see, for example, Refs. 1-3) they generally assume an "ideal" skirt material behavior.[2-4] This ideal is an inelastic massless membrane incapable of sustaining any compressive stress. There is, however, very little available on the effect of the

Presented as Paper 83-0369 at the AIAA 21st Aerospace Sciences Meeting, Reno, Nev., Jan. 10-13, 1983; received March 19, 1984; revision received Aug. 20, 1984.

*Research Engineer, Institute of Aerospace Studies. Student Member AIAA.
†Professor, Institute of Aerospace Studies. Associate Fellow AIAA.
‡Research Associate, Institute of Aerospace Studies; presently with Memorial University, St. John's, Canada. Member AIAA.

skirt material properties on dynamics, both for full-scale vehicles and in terms of the scaling requirements for models. The work described here shows that the viscoelastic properties of two materials used in the writers' laboratory to build model skirts have major effects on the dynamics. This occurs because small deformations in the skirt can interact strongly with the dynamics by causing large changes in both the hovergap and the effective pneumatic capacitance of the cushion volume. This raises fundamental questions about the scaling of model skirts, as well as about the significance of skirt material properties at full scale.

The role of skirt extensibility in ACV dynamics was first considered by Ribich and Richardson[5] in 1967, who undertook an analytical investigation of a guided ground vehicle configuration. They also identified the key role played by the compressibility of the air in the cushion volume: it is the basic source of dynamic instability. However, they used a purely elastic model, and indications that this may be insufficient have come from several sources. Sullivan[6] described uniaxial tension tests of typical skirt materials, which showed that the stiffness depends strongly on strain rates, and Hinchey[7] and Cox[8] have noted that predicted test model behavior can be very underdamped relative to that experimentally observed.

Large differences in the dynamics of model skirts attributable directly to material properties have been observed at the writers' laboratory.[4,9-11] For example, a 2.44×1.22-m planform model of an uncompartmented, segmented skirt was found to be subject to a combined pitch/heave dynamic instability when equipped with segments made from an 0.10-mm-thick urethane-coated nylon fabric, for which $w_s = 0.076$ kg/m^2 and $C_{SW} = 0.0054$. For segments made from 0.13-mm-thick extruded polyethylene film, with $w_s = 0.118$ kg/m^2 and $C_{SW} = 0.0083$, the motion was always heavily damped. Measurements of static pitch and roll stiffness for this model with the nylon-urethane segments installed agreed closely with a theory based on the ideal model material concept.[10,11] In contrast, the polyethylene segments generate large hysteresis of a type observed by the authors for other geometries.[4,9] This hysteresis has been attributed to sliding friction between the segments and the ground[13] and to localized buckling generated by skirt/ground contact.[12] Experiments by the authors indicate that both mechanisms can occur.[4,9] Corresponding skirt material effects on both the dynamic stability and hysteresis in roll and pitch stiffness have been observed on a 4.08×2.06-m, 850-kg test model at the authors' laboratory.[10,11]

The marked differences in the dynamics caused by these model materials emphasized the need for an investigation of their effect on the dynamics of a simple cushion configuration that was already well understood. The configuration chosen for this investigation is depicted in Fig. 1; it is a single plenum chamber free to move in heave only with its air supplied from a large pressurized spherical reservoir by a moderately long duct. This apparatus completely uncouples the dynamics of the air supply system from that of the model being tested and provides an ideal constant-pressure source of air. Information on the dynamical properties of a cushion system is obtained by observing the effect of various parameters such as cushion weight and cushion volume flow on dynamic stability. Although cushion dynamics can be highly nonlinear, particularly when skirt/ground contact occurs,[3,14,15] it has been found that this configuration accurately reproduces the stability predictions of a linear analysis for a rigid plenum chamber.[14,16]

The present work extends the analysis of Ref. 16 to include the effects of the viscoelastic properties of the two materials discussed above on the dynamics of a flexible skirt installed in the apparatus depicted in Fig. 1. The geometry chosen for the skirt is an inverted, slightly tapered cone; it is perhaps the simplest that retains the essential properties of an amphibious flexible skirt, these are: a geometry stabilized by the cushion pressure and a flexible bottom edge or lip. Oscillatory uniaxial tension and stress relaxation tests were used to obtain data on the viscoelastic properties of the 0.10-mm nylon-urethane and 0.13-mm polyethylene materials. These data were in turn used to specify the phenomenological material models for prediction of the effect of cushion pressure on cushion volume and hovergap. The extended stability analysis was then used to demonstrate the effects of the material properties on stability for ranges of the material parameters that might be expected in model skirts, and to predict the effect of the two materials on the stability of the duct/plenum system shown in Fig. 1. The second set of predictions is compared with results of experiments.

Comments on the Properties of Skirt Materials

Both components of ACV skirt material, the woven fabric and its elastomer coating, are usually manufactured from polymers. These substances can have complicated structural properties; typically, they exhibit highly nonlinear stress-strain relationships, which can depend strongly on temperature, stress histories, and strain rates or excitation frequencies in the case of oscillatory loading. They can also be subject to substantial creep and stress relaxation.[17,18] One phenomenon of direct interest here is the existence of a range

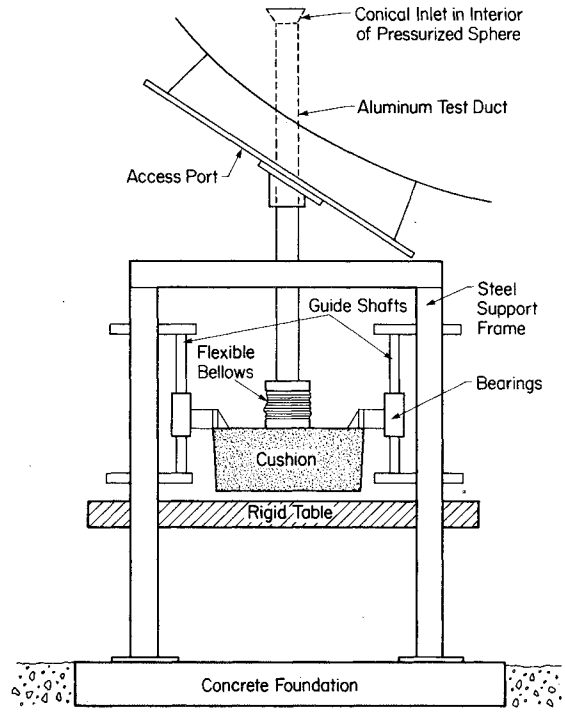

Fig. 1 Dynamic stability experiment used in the present investigation.

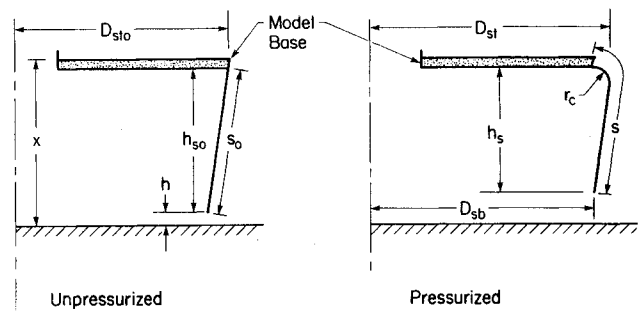

Fig. 2 Undeformed and deformed geometry of conical cells. In all cases $D_{st0} = 0.508$ m, $D_{in} = 0.127$ m, and $h_{s0} = 0.213$ m. For the rigid skirt $D_{sb0} = 0.467$ m, for the polyethylene $D_{sb0} = 0.469$, and for the nylon-urethane $D_{sb0} = 0.473$.

of excitation frequencies, below which the material can have a very low elastic modulus and is said to be "rubbery" and above which the elastic modulus may be several orders of magnitude higher and the material is said to be "glassy." In the transition regime, the material may be highly viscoelastic, whereas in both the rubbery and glassy regimes the elastic modulus is independent of frequency and the viscous effects are usually small. For structural analysis, this behavior is modeled by series and parallel combinations of equivalent springs and dashpots.[17,18] The choice of combination depends on the aspect to be modeled and the accuracy required. Samples taken from full-scale vehicles have shown a single transition[6] that can be reproduced, qualitatively at least, by the standard linear model. This model and the Voigt model were used in the calculations described below.

An additional problem in characterizing ACV skirt material is that, since the major structural element is a woven fabric, properties peculiar to this type of construction have to be considered. The weaving process can bend the individual fibers considerably, so that the basic stiffness of a fabric is initially low but increases as the fibers straighten under load.[19] Also, the initial stiffness in the warp fiber direction is usually much higher than in the fill fiber direction. Furthermore, the effective stiffness in directions not close to either fabric direction may be very low. These orthotropic properties together with the viscoelastic effects make the task of analysis of loads and deformation of practical skirt geometries very difficult. The basic reason for the choice of a slightly tapered cone for the present work is that many of these difficulties are minimized.

Dynamic Stability Analysis

The principal geometric quantities used in the analysis are depicted in Figs. 1 and 2. The elements of the theory are as follows. The sphere provides a source of air at constant pressure p_f. The flow through the conical inlet from the sphere to the duct entrance is assumed to be quasisteady and governed by Bernoulli's law:

$$Q_d = C_{mi} A_d [2(p_f - p_{df})/\rho]^{1/2} \tag{1}$$

Pressure gradients along the duct are assumed to arise only from the unsteady inertia of the air,[14] in which case

$$\frac{dQ_d}{dt} = \left(\frac{A_d}{\rho L_d}\right)(p_{df} - p_c) \tag{2}$$

The compression process in the cushion volume V_c is assumed to be isentropic so that for low p_c, application of the continuity principle to the cushion volume leads to the equation

$$C_c\left(\frac{dp_c}{dt}\right) + \frac{dV_c}{dt} = Q_d - Q_a \tag{3}$$

The air escape process from the cushion volume is also assumed to be governed by the same law as for the inlet:

$$Q_a = C_m \ell_s h (2p_c/\rho)^{1/2} \tag{4}$$

The heave dynamics is assumed to be governed by Newton's law for a single rigid mass:

$$(W/g)\,d^2x/dt^2 = S_a p_c - W \tag{5}$$

For a rigid skirt, $x = h_s + h$, $V_c = V_d + S_a h$, and the formulation is complete.

The formulation for a flexible skirt requires a description of the effects of skirt deformation on S_a, ℓ_s, V_c, and h_s under the action of p_c (t) as depicted in Fig. 2. To calculate these quantities, it is assumed that, except for a small region in the neighborhood of the top, the deformed skirt remains conical. To calculate h_s, it is assumed that the top of the conical portion, which has diameter D_{st}, is connected to the base of the model by a segment of material having a circular cross section of radius $r_c = (D_{st} - D_{st0})/2$. This shape change causes a shortening of the skirt

$$\Delta h_{sl} = (\pi/2 - 1) r_c \tag{6}$$

In the conical portion, the longitudinal stress varies from zero at the bottom to a maximum of twice the mean stress

$$\sigma_{\ell m} = p_c (D_{st} - D_{sb})/4t_s \tag{7}$$

For values of the skirt taper angle θ used in the present work, $\sigma_{\ell m}$ is usually less than 5% of σ_h, so that its effect on the hoop deformation of the conical portion is ignored. The overall effect of p_c in shortening the skirt by an amount $\Delta h_s = h_{so} - h_s$ can be expressed as a contraction ratio $\nu_e = (\Delta h_s \ell_{s0})/(\Delta \ell_{s0})$, which is taken to be the sum of three terms;

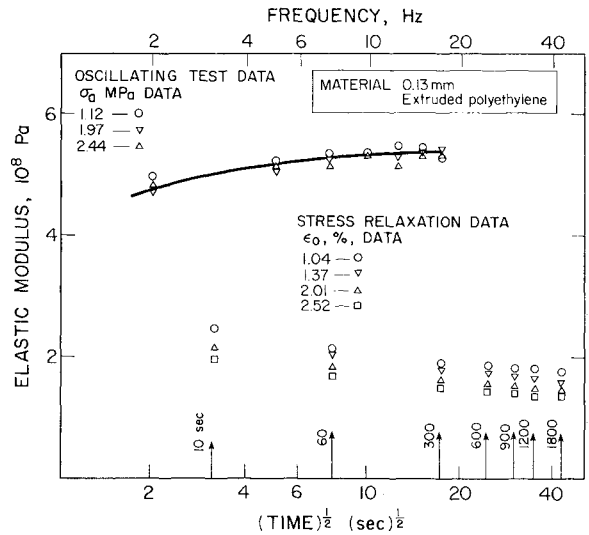

Fig. 3 Dynamic stiffness and stress relaxation data for polyethylene.

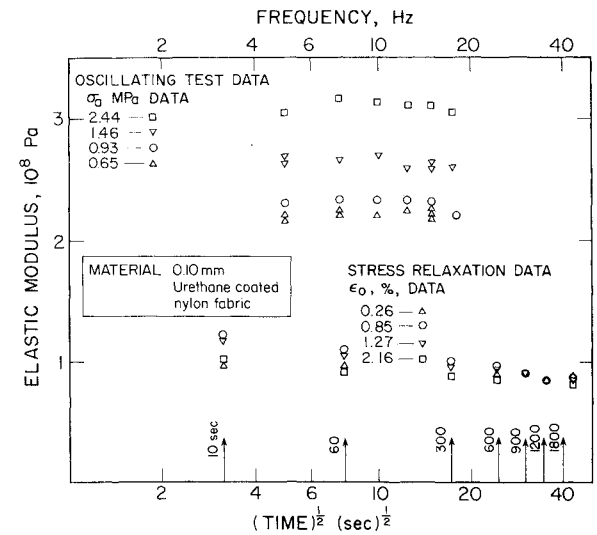

Fig. 4 Dynamic stiffness and stress relaxation data for nylon-urethane fabric at 90 deg to warp direction.

with $\epsilon^* = (\ell_s - \ell_{s0})/\ell_{s0}$,

$$\nu_e = \nu_h + (\Delta h_{s1} - \Delta h_{s2})/(h_{s0}\epsilon^*) \tag{8}$$

In this expression ν_h is the Poisson's ratio associated with hoop deformation, Δh_{s1} is given by Eq. (6), and Δh_{s2} is the extension caused by longitudinal stresses. The quantity ν_e may be considered as an equivalent Poisson's ratio and, for the values of θ used here, the third term is very small compared to the other two.

The final forms of the expressions for S_a, ℓ_s, V_c, and h depend on the viscoelastic material model adopted. For the standard linear model, after some algebra, one obtains

$$S_a = \ell_s^2 d_r^2/4\pi - A_d \tag{9}$$

$$\eta \frac{\mathrm{d}}{\mathrm{d}t}\left[\frac{p_c \ell_s}{2\pi t_s E_g} - \epsilon^*\right] = E_v \epsilon^* - \left[1 + \frac{E_v}{E_g}\right]\frac{p_c \ell_s}{2\pi t_s} \tag{10}$$

$$V_c = \frac{h\ell_s^2 d_r^2}{4\pi} + \frac{h_{s0}}{12\pi}[1 - \nu_e \epsilon^*]\ell_s^2 (d_r^2 - 2d_r + 4) \tag{11}$$

$$h = x - [1 - \nu_e \epsilon^*] h_{s0} \tag{12}$$

To determine the stability of this system of equations, standard linear analysis procedures are used. When these equations are linearized about a given equilibrium operating point, p_{ce} and Q_e, the linearized system is grouped in the matrix form $\boldsymbol{A}\dot{x} = \boldsymbol{B}x$ where, for a standard linear material model, the system is of sixth order and $x = [\Delta p, \Delta h, \Delta \dot{h}, \Delta Q_d, \Delta \ell_s, \Delta \dot{\ell}_s]^T$. Stability is determined by direct examination of the system eigenvalues, which for given p_{ce} and Q_e are determined numerically.[20] For the materials used in the tests and in the comparative studies, the analysis showed that the oscillation frequencies lay in a narrow range of about 12-16 Hz. This simplified the task of characterization of the materials.

Skirt Material Properties

In the oscillatory tension tests, a servo-controlled hydraulic ram was used to impose small-amplitude deformation oscillations at several levels of mean deformation on the samples for frequencies in the range of 2-17 Hz.[20] The load response of the sample was obtained by a piezoelectric load cell and the resultant data were expressed in terms of the complex modulus concepts of storage modulus E_1 and loss angle δ.[17] The same apparatus was used to impose step deformations for the stress relaxation data. The principal results are given in Figs. 3 and 4 and Table 1. Data were obtained for material samples taken at 0 and 90 deg to the extrusion direction in the polyethylene material and at 0 and 90 deg to the warp direction of the nylon-urethane material.

Figure 3 gives E_1 as a function of frequency for polyethylene at the 90 deg orientation for three stress levels and the corresponding stress relaxation data for four initial strains. A stress $\sigma_h = 2.5$ MPa corresponds to a cushion pressure of about 1 kPa for the present cell geometry and is representative of that used in the experiments. The most noticeable feature is that, at frequencies of 2 Hz and above, E_1 is larger than the stress relaxation values by a factor of about 2.5. It is also independent of the stress and is a slowly increasing function of frequency. The stress relaxation data also show significant decreases of modulus with time and, for the data at each time point there is a small but consistent trend of decreasing modulus with increasing strain. Thus, the value of the static modulus quoted in Table 1 is an average and is based on the load at 20-min elapsed time. This interval was chosen because it was representative of the times involved in the experiment. The data for the 0-deg orientation is essentially the same as for the 90-deg orientation.

Figure 4 gives data on E_1 for nylon-urethane samples oriented at 90 deg to the warp direction; this was the orientation of the hoop direction in the model tests. E_1 is effectively independent of frequency, but it increases substantially with increases in σ. E_1 is also substantially above the values of E determined in the stress-relaxation tests. It was found that the stress-relaxation properties of this material are critically dependent on the recent stress history. In a series of measurements in which the initial strain was increased in steps monotonically, the resultant force histories usually differed greatly from those obtained by allowing the sample to recover at zero stress for a period equal to the test period before proceeding to the next strain increment. The data given in Fig. 4 were obtained from monotonically increasing strains, since this corresponds to the way in which the stability experiments were performed. Table 1 gives estimates of the 20-min value of E for the data plotted in Fig. 4, in which no resting or recovery was allowed, and values of E with recovery. The latter values of E were much more stress dependent and close to the value of E_1. Also, as shown in Table 1, the values of E and E_1 for a sample cut parallel to the warp direction, although higher than those for the 90-deg sample, are roughly equal.

Loss angles for both materials are small and for the nylon-urethane are negligible. However, those of the polyethylene decrease almost linearly with the increase in frequency changing from about 7.5 deg at 2 Hz to 2 deg at 17 Hz; this behavior and that for E_1 in Fig. 3 are consistent with that of a standard linear model at frequencies approaching a glassy region.

Estimates of the static Poisson's ratio for the two materials were obtained by placing sharp-edged grid patterns on the samples, and then photographing them in the stressed and unstressed state. The changes in grid length were obtained by examining the negatives in a universal measuring projector. The results are given in Table 1; however, it should be noted

Table 1 Summary of material properties

Material	Thickness, mm	Static modulus E, Pa	Dynamic properties: Storage modulus[a] E_1	Dynamic properties: Loss angle[a] δ, deg	Dynamic properties: Poisson's ratio
Aluminum	1.58	6.9×10^{10}	—	—	0.33
Polyethylene at 0 and 90 deg	0.127	1.5×10^8	5.4×10^8	2	0.3
Nylon-urethane 0 deg to warp	0.102	6.25×10^8	$6.52 \times 10^8 + 49.4\sigma$	<0.5	—
Nylon-urethane 90 deg to wrap		No recovery: 0.87×10^8	$1.84 \times 10^8 + 51.8\sigma$	<0.5	0.75
		Recovery: $1.60 \times 10^8 \times (1 + 10^{-7}\sigma + 10^{-14}\sigma^2)$			

[a] Values of E_1 and δ are quoted for a frequency of 15 Hz, which is the average of measured frequencies in test model.

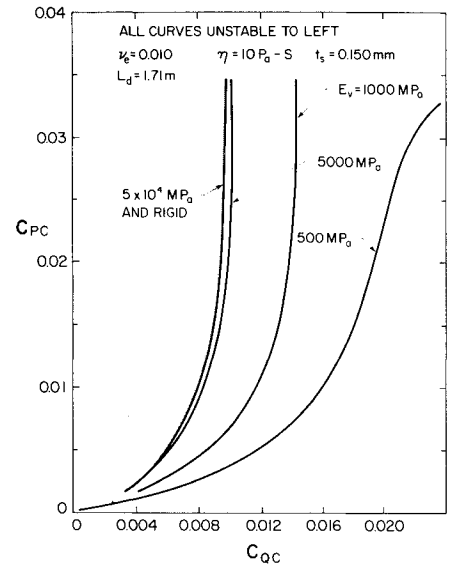

Fig. 5 Predicted effect of elastic modulus on dynamic stability.

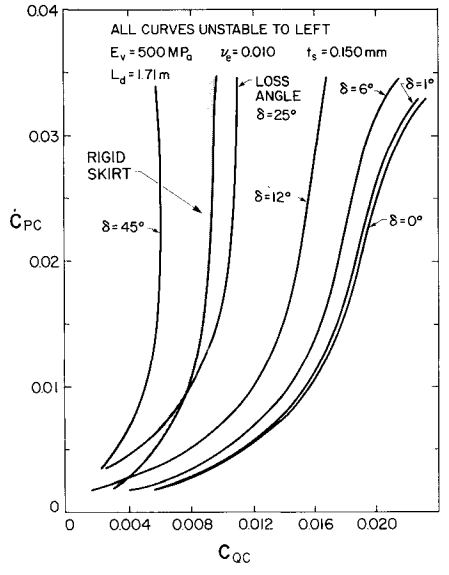

Fig. 6 Effect of loss angle on dynamic stability.

that these measurements are subject to large errors, possibly 50% and higher, and ultimately an improved technique will have to be developed.

Predicted Effects of Skirt Material Properties on Stability

The stability characteristics of the duct-plenum model are presented in the form of stability boundaries, which are plotted in terms of nondimensional equivalents of the two quantities of basic design interest, p_{ce} and Q_e,

$$C_{PC}=p_{ce}/P_a, \quad C_{QC}=Q_e(\rho/2WA_b)^{1/2} \tag{13}$$

The quantity C_{QC} scales cushion flow rates for model tests and the range $0.001<C_{QC}<0.02$ is representative of full-scale values.[21] The dimensions of the model used in the calculations are those used in the experiment, which utilizes a 0.0779 m diameter supply duct with a friction factor of 0.01656 and cushions of the geometry given in Fig. 2. Hinchey[7] has shown that, for a family of directly fed geometrically similar cells, the effect of cell size on the value of C_{PC} at instability enters only through C_{QC}. If a duct is present, this similitude is preserved approximately. Hence, qualitatively at least, the results apply to larger geometries.

Predictions of the effect of material parameter changes on stability are given in Figs. 5-7, and stability boundaries for the two skirt materials used in the experiments are given in Fig. 8. In each case the stability boundary corresponding to an inelastic skirt is used as a reference condition. Figure 5 shows typical elastic modulus effects, which were obtained with a Voigt model because $E_l=E_v$ and is thus independent of frequency.[17] Also, both η and ν_e were given very small values to eliminate both the material loss and contraction effects on V_c and h_s. The results show that materials having $E_v=500$ MPa or less, which is representative of those used in the experiments, cause large departures from the corresponding boundary for an inelastic skirt. Since the curves in Fig. 5 are unstable to the left, the elasticity has a large destabilizing effect. The effect of the material damping was also examined by using a Voigt model, with the quantities E_v and t_s assigned representative values and ν_e kept small. The results in Fig. 6 show a stabilizing effect; in fact, for large enough values of δ, the inelastic boundary is crossed. Values of $\delta=25$ deg and higher can be expected for materials operating at frequencies in the transition between the rubbery and glassy regimes.[17]

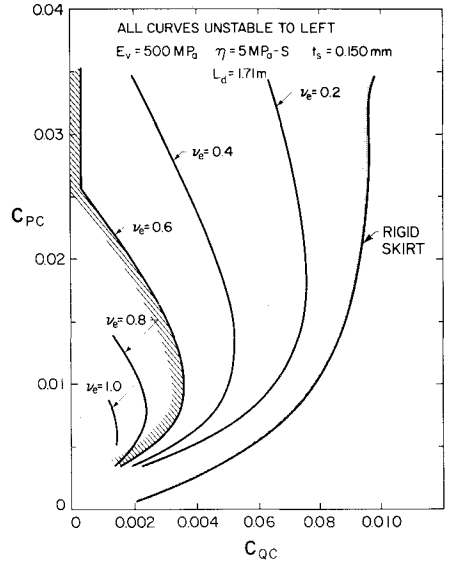

Fig. 7 Effect of skirt contraction on dynamic stability.

Variation of skirt thickness also affects the stability through Eq. (10). An increase in t_s usually increases stability, but at large loss angles a destabilization can occur.

Figure 7 shows the predicted effect of skirt contraction ratio; a Voigt material model was again used. The effect of increasing ν_e is twofold: it both increases h and reduces V_c. For a cylinder the perturbation in volume owing to a hoop strain ϵ_h is $\delta V_c/V_c=(2-\nu_e)\epsilon_h$ to first order, so that for values of $\nu_e<2$, there is still an increase in V_c associated with hoop deformation. In general, the effect of increasing the skirt contraction is stabilizing, since the curves are moved to the left. This must be associated with the modulation of the hovergap, since the effect occurs for values of $\nu_e<2$. The curves also display a feature not present in the results for an inelastic skirt or those for an elastic skirt undergoing changes only in V_c. For a given stability boundary and for large enough ν_e, as p_{ce} increases from zero, the slope dQ_e/dp_{ce} of the boundary is at first positive and then becomes negative and crosses $Q_e=C_{QC}=0$. This is shown for $\nu_e=0.6$ in Fig. 7. This implies that, in the absence of contraction effects on hovergap for any given W or p_{ce}, there is always a value of Q_e below which the system is dynamically unstable. However, for

$\nu_e > 0$, above a certain critical p_{ce} the system can be dynamically stable for all Q_e. Clearly, the presence of such an effect in the experimental results provides a critical test of the present theory. Of course, at $Q_e = 0$, the system becomes statically unstable, because a plenum chamber cushion requires $Q_e > 0$ to have a positive stiffness. The presence of this static instability is illustrated for $\nu_e = 0.6$ in Fig. 7 by the cross hatching along the C_{PC} axis.

Predicted results with mean values for static and dynamic stiffnesses, loss angles, and contraction coefficients of skirt materials used in the experiments are given in Fig. 8. In all cases, a standard linear model was used for the stability calculations. The results show large deviations from the inelastic boundary for both materials, especially for values of p_{ce} above 1 kPa. Also, for the nylon-urethane material oriented at 90 deg, the intersection of the stability boundary with $Q_e = 0$ occurs at values of p_{ce} well within the range attainable in the experiments.

Stability Experiments

Apparatus and Method

Since the hoop direction of a conical surface becomes a circular arc when developed, it cannot be aligned with one of the fiber directions of a fabric. The impact of this problem was minimized by building the cells from four sectors of fabric, so that for $\theta = 5.5$ deg the hoop direction deviated from the fabric direction a maximum of 4 deg. An estimate of the reduction in the mean hoop stiffness, made by counting the fraction of fibers that were not continuous from one side of the sector to the other, indicated that the effect should be less than 1%.

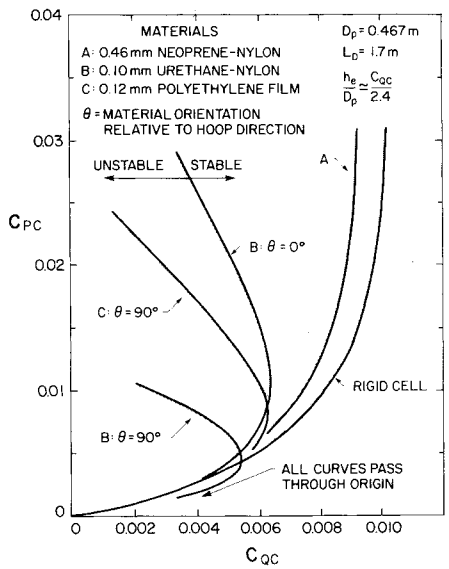

Fig. 8 Dynamic stability boundaries for the polyethylene and nylon-urethane materials.

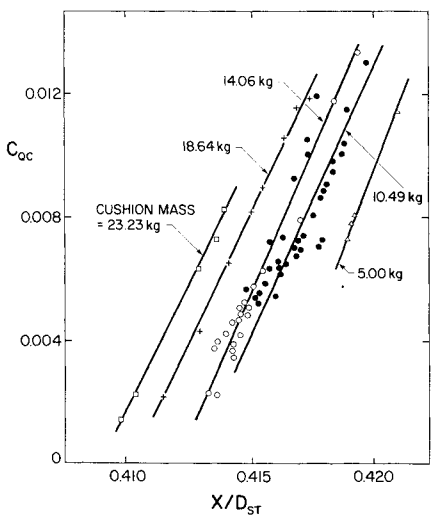

Fig. 9 Cushion flow function for nylon-urethane material.

In a given experiment, the required p_{ce} is obtained by attaching calibrated weights to the top of the cushion and the required Q_e is set by using a blowoff valve to adjust the pressure in the sphere. The value of Q_e is measured by the conical inlet, which was calibrated in situ by an ASME standard orifice plate meter[22] inserted prior to final installation of the model cushion. A baffle plate is located in the cushion to break up the flow from the duct and the static pressure is measured by two taps in the cushion base plate located to the sides of this baffle plate. A Shaevitz model 5000HR displacement transducer is used to measure the cushion height above the table.

For the materials used in these experiments, it proved to be very difficult to trim the bottom edge of the cell to obtain a visually uniform hovergap. This problem was circumvented as follows. For any flexible skirt installed in the apparatus, including one in which parts of the periphery are touching the table, the flow is still expected to be orifice-like, but there may be an irregular orifice area and a discharge coefficient that are functions of x, and of p_{ce} if skirt deformation is significant. Hence, dimensional considerations imply that

$$C_{QC} = f_\ell [x/D_{st},\ (p_{ce}D_{st}/Et_s)] \tag{14}$$

and, if the flow is governed by Bernoulli's law, the "flow function" f_ℓ should be independent of p_{ce} in the absence of skirt deformation. In general, this function can be linearized and incorporated in the stability analysis; however, if the dependence on x is linear, it can then be used to obtain an equivalent hovergap. This was shown to be the case for the results described below.

Finally, the dynamic stability at a given p_{ce} and Q_e is determined by the simple expedient of manually disturbing the cushion and observing the subsequent motion, be it growth to limit cycle oscillations[3,15] or decay to equilibrium. This experimental configuration was tested with an inelastic skirt and it was shown[15] that the test method, although potentially subject to considerable error, yielded highly repeatable boundaries in close agreement with the linear theory predictions. Moreover, the ±4% accuracy obtained in C_{QC} was as good as that from a technique based on the determination of oscillation damping at various Q_e in the stable region and finding the critical value of Q_e by extrapolating these data to zero damping. Also, the location of the predicted stability boundaries using the numerical solution of the nonlinear equations with finite initial displacements of up to 100% of h_e yielded results in close agreement with the linear theory.[16] Hinchey[7] has suggested that this occurs because at the stability boundaries the real parts of the eigenvalues of the linear system matrix are rapidly varying functions of p_{ce} and Q_e, a situation not true for all ACV configurations.[23]

Results and Discussion

A typical flow function for the nylon-urethane skirt is given in Fig. 9. It shows a strong dependence on W; in contrast, the polyethylene skirt displayed no detectable dependence on W. Linear regression was applied to the data in Fig. 9 to obtain an estimate of C_m as a function of p_{ce}, which was used in the theoretical predictions. The measured values of C_m for both skirts are quoted with the appropriate figures. The data in Fig. 9 were used to obtain an estimate of ν_e for the static case; for a representative value of C_{QC}, $\nu_e = 1.9$, which compares with the value 1.4 determined from Eq. (8).

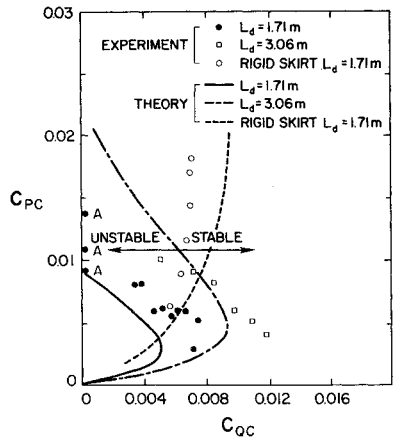

Fig. 10 Comparison of theory and experimental results for nylon-urethane skirt and two duct lengths. For rigid skirt $C_m = 0.60$ and for nylon-urethane $C_m = 0.591\text{-}0.147 \times 10^{-3} p_c$.

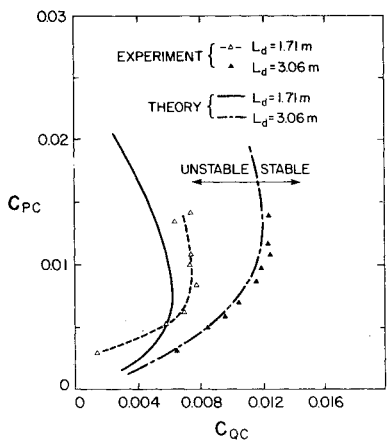

Fig. 11 Comparison of theory and experimental results for polyethylene skirt and two duct lengths, $C_m = 0.53$.

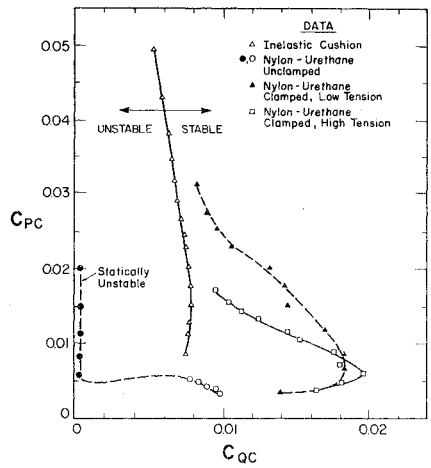

Fig. 12 Effect on stability using clamp to prevent skirt contraction. (All curves are unstable to the left.)

It was found that, apparently owing to creep, the position of the stability boundary depended on the previous stress history and the amount of time the cushion was loaded with the particular weight being tested. This effect was most pronounced for the nylon-urethane skirt; it produced changes of up to ±17% in the value of C_{QC} at a stability boundary, as is shown by the data at C_{PC} near 0.006 in Fig. 10. To counter this effect in the subsequent stability boundary tests, the cushion was allowed to condition at the test pressure approximately 15 min.

The stability boundaries for the two skirt materials are compared with theory in Figs. 10 and 11. The theory and experiment for the rigid skirt with $L_d = 1.71$ m are included in Fig. 10.[14] For the nylon-urethane skirt, the theory incorporated its nonlinear stress-strain relationship; at a given p_{ce} the hoop stress was calculated and the formulas given in Table 1 were used to compute the equilibrium strain and to estimate a local elastic modulus for small deviations in the strain about equilibrium. This local modulus was used in a Voigt model of the material for the stability analysis. Considering the various difficulties discussed above, good qualitative agreement between theory and experiment for both materials has been obtained; in particular, both the marked shift from the rigid-skirt data and the slope reversal associated with skirt contraction are present for the nylon-urethane data at the two duct lengths. Furthermore, the experimental data for $L_d = 1.71$ m showed clear evidence of the intersection of the dynamic stability boundary with $C_{QC} = 0$ at about $C_{PC} = 0.009$. For the three points labeled A in Fig. 10, which correspond to values of C_{QC} less than about 0.0002, the cushion simply collapsed under its own weight, as is characteristic of a static instability.[24] The major source of the discrepancy between theory and experiment for the nylon-urethane skirt probably lies in the measurements of Poisson's ratio ν and the estimation of ν_e.

Finally, a demonstration of the opposing effects on the stability of skirt contraction and hoop extension was obtained by a simple modification of the experiment. A clamp that prevented skirt contraction but still permitted hoop deformation was installed. It was a ring of outer diameter D_{sb} supported at the bottom of the skirt by rods attached to and extending downward from the model base. The lip of the flexible skirt was clamped to this ring and a substitute rigid lip was attached to the bottom of the ring. According to the theory, the use of such a clamp should eliminate the critical C_{PC} above which the system becomes dynamically stable near $Q_e = 0$ and should shift the dynamic stability boundary to the right of the inelastic boundary. The data obtained by using this clamp are given in Fig. 12; it clearly confirms these predictions. However, note that the boundaries for the clamped skirt do not have the shape predicted in Fig. 5. Instead they approach the inelastic boundary as C_{PC} increases. Presumably this is a result of the tendency of a fabric to stiffen as it is loaded.

Conclusions

The large departure of the dynamic stability characteristics of a model air cushion skirt from those for an ideal skirt material, predicted for two laboratory model materials, have been confirmed by the experiments. An interesting feature of the results is the way in which the urethane-coated nylon fabric, which for static pitch and roll stiffness was effectively ideal, caused the largest departures from this ideal in the dynamic experiments. It occurred because small deformations of the skirt material, which may not be very significant in vehicle static behavior, have large effects on the cushion hovergap history and pneumatic capacitance. In contrast, the extruded polyethylene material, which in static pitch and roll experiments generated large hysteresis, was closer to ideal in its dynamic behavior. This tends to reinforce an earlier conclusion that the hysteresis is associated with local buckling phenomena, triggered by skirt/ground contact.

Finally, it should be reaffirmed that, since dynamic stability is but one manifestation of the dynamical properties of a cushion system, the conclusions drawn here are relevant to other dynamics problems. For example, the implication for the testing of physical models of practical configurations is that great care may have to be exercised in the choice of model material—otherwise, spurious results may be obtained.

Acknowledgments

The work was made possible by a series of contracts awarded by the Government of Canada's Transportation Development Centre. The work was also supported by the Natural Sciences and Engineering Research Council of Canada through Grant A3378. The assistance of Mr. G. C. Remillard in performing some of the experiments is acknowledged.

References

[1] Doctors, L. J., "Nonlinear Motion of an Air Cushion Vehicle over Waves," *Journal of Hydronautics*, Vol. 9, April 1975, pp. 49-57.

[2] Carrier, R., Magnuson, A. H., and Swift, M. R., "Seakeeping Dynamics of a Single Cushion Peripheral Cell-Stabilized Air Cushion Vehicle," *Journal of Hydronautics*, Vol. 12, April 1978, pp. 49-54.

[3] Hinchey, M. J. and Sullivan, P. A., "A Theoretical Study of Limit Cycle Oscillations of Plenum Air Cushions," *Journal of Sound and Vibration*, Vol. 79, No. 1, Nov. 1981, pp. 61-77.

[4] Sullivan, P. A., Hinchey, M. J., and Delaney, R. G., "Static Roll Stiffness Characteristics of Two Multicell Type Air Cushion Systems," *Journal of Terramechanics*, Vol. 15, No. 1, March 1978, pp. 15-41.

[5] Ribich, W. A. and Richardson, H. H., "Dynamic Analysis of Heave Motion for a Transport Vehicle Fluid Suspension," Dept. of Mechanical Engineering, Massachusetts Institute of Technology, Boston, Rept. DSR-76110-3, Jan. 1967.

[6] Sullivan, P. A., "The Air Cushion Technology Program at the University of Toronto," *Canadian Aeronautics and Space Journal*, Vol. 20, June 1974, pp. 269-286.

[7] Hinchey, M. J., "Heave Instabilities of Amphibious Air Cushion Suspension Systems," Institute for Aerospace Studies, University of Toronto, Canada, Rept. 246, Nov. 1980.

[8] Cox, R. J., "Measurements of the Dynamic Response of a Hovercraft Model to Waves of Various Lengths Using the Whirling Arm Facility," College of Aeronautics, Cranfield Institute of Technology, Bedford, England, Aero Rept. 7803, Nov. 1977.

[9] Sullivan, P. A., Hinchey, M. J., Murra, I., and Parravano, G. J., "Research on the Stability of Air Cushion Systems," Institute for Aerospace Studies, University of Toronto, Canada, Rept. 238, Sec. 3, pp. 25-35, Nov. 1979.

[10] Sullivan, P. A., Hinchey, M. J., Hartmann, P. V., Dupuis, A., Green, G. M., and Graham, T. A., "Research Into Air Cushion Stability," 1979 Report, Transportation Development Centre, Montreal, Rept. TP3109E, Sec. 3, pp. 50-99, Jan. 1982.

[11] Sullivan, P. A., Hartmann, P. V., and Graham, T. A., "Application of System Identification Flight Analysis Techniques to the Pitch-Heave Dynamics of an Air Cushion Vehicle," *Canadian Aeronautics and Space Journal, Transactions*, Vol. 29, No. 4, Dec. 1983, pp. 348-370.

[12] "Stability and Control of Hovercraft: Notes for Commanders," United Kingdom Dept. of Industry, Ship and Marine Technology Requirements Board Report, 1980.

[13] Lee, E. G. S. et al, "Experimental and Analytical Studies of Advanced Air Cushion Landing Systems," NASA CR NAS-7723.5-3, Aug. 1981.

[14] Sullivan, P. A., Hinchey, M. J., and Green, G. M., "A Review and Assessment of Methods for the Prediction of the Dynamic Stability of Air Cushions," *Journal of Sound and Vibration*, Vol. 84, No. 3, Oct. 1982, pp. 337-358.

[15] Sullivan, P. A., Byrne, J. E., and Hinchey, M. J., "Nonlinear Heave Dynamics of a Simple Flexible Skirt Air Cushion," to be published in *Journal of Sound and Vibration*.

[16] Hinchey, M. J. and Sullivan, P. A., "Duct Effects on the Heave Stability of Plenum Air Cushions," *Journal of Sound and Vibration*, Vol. 60, No. 1, Sept. 1978, pp. 87-99.

[17] Ward, I. M., *Mechanical Properties of Polymers,* John Wiley and Sons, New York, 1971, p. 95.

[18] Aklonis, J. J., MacNight, W. J., and Shen, M. C., *Introduction to Polymer Viscoelasticity*, Wiley Interscience, New York, 1972.

[19] Minami, H. and Hakahara, Y., "An Application of the Finite Element Method to the Deformation Analysis of Coated Plain Weave Fabrics," *Journal of Coated Fabrics*, Vol. 11, April 1981, pp. 310-327.

[20] Graham, T. A., "The Effects of Skirt Material Choice on the Heave Stability of an Air Cushion," M.A.Sc. Thesis, Institute for Aerospace Studies, University of Toronto, Canada, Nov. 1980.

[21] Fowler, H. S., "On the Lift-Air Requirement of Air Cushion Vehicles and Its Relation to the Terrain and Operational Mode," Div. of Mechanical Engineering, National Research Council of Canada, Rept. ME-246, May 1979.

[22] *Flow Meter Computation Handbook*, American Society of Mechanical Engineers, New York, 1961.

[23] Hinchey, M. J., Sullivan, P. A., and Dupuis, A. D., "Heave Dynamics of Large Air Cushion Platforms," *Journal of Sound and Vibration*, to be published.

[24] Huseyin, K., *Vibrations and Stability of Multiple Parameter Systems,* Noordhoff, Alphen Aan Den Rijn, the Netherlands, 1978, p. 50.